Entanglement in finite spin rings with noncollinear Ising interaction

F. Troiani
Istituto Nanoscienze-CNR, S3, Modena, Italy
(Dated: December 21, 2010)

We investigate the entanglement properties of finite spin rings, with noncollinear Ising interaction between nearest neighbours. The orientations of the Ising axes are determined either by the spin position within the ring (model A) or by the direction of the bond (model B). In both cases, the considered spin Hamiltonians have a point group symmetry, rather than a translation invariance, as in spin rings with collinear Ising interaction. The ground state of these models exhibit remarkable entanglement properties, resembling GHZ-like states in the absence of an applied magnetic field (model B). Besides, the application of an homogeneous magnetic field allows to modify qualitatively the character of the ground state entanglement, switching from multipartite to pairwise quantum correlations (both models A and B).

PACS numbers: 03.67.Bg,75.10.Jm,75.50.Xx

I. INTRODUCTION

Spin rings represent prototypical low-dimensional systems with highly entangled ground states [1, 2]. In particular, antiferromagnetic and isotropic exchange interaction induces pairwise entanglement between nearest-neighbouring spins; moreover, it maximizes the concurrence within the set of translationally invariant states with vanishing magnetization [3]. Quantum entanglement in anisotropic Heisenberg models has also been investigated, partly in relation to the separability of the ground state for specific values of the applied magnetic field [4–10]. Indeed, the magnetic field can be used as a control parameter in order to engineer the ground state and thermal entanglement of the system. The interplay between the system anisotropies and the field offer even wider possibilities if one assumes that this needs not be homogeneous, but can rather be controlled locally [6, 11, 12].

Previous analyses were mainly devoted to systems with translational invariance, where the anisotropies in the spin-spin couplings are independent on the site. However, physical implementations of low-dimensional spin systems are typically characterized by point-group symmetries, rather than traslational invariance [13]. This is the case, for examples, of nanomagnets [14], that represent a rich class of molecular spin clusters, with widely tunable geometries and physical parameters. A number of ring-shaped nanomagnets has been investigated in the last years [14]; some of these possesses attractive features for the encoding and manipulation of quantum information [15–17]. In this paper we consider rings formed by equivalent spins, where the anisotropies in the spin-spin couplings reflect the point-group symmetry of the molecule and the local environment of each spin. In particular, we focus on spin models with noncollinear Ising interaction between nearest neighbours [18, 19]. The resulting spin Hamiltonians don't fall into any of the commonly considered cases and - unlike the standard Ising model - can exhibit highly entangled ground states, also in the absence of an applied magnetic field.

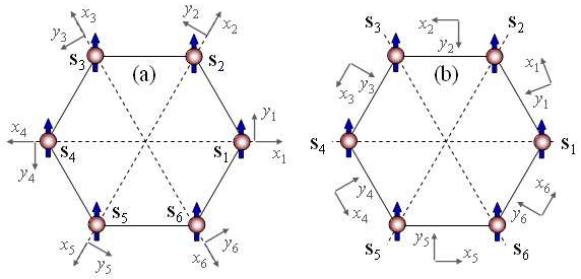

FIG. 1: (color online) Twisted-spin representations of an hexagonal spin ring. (a) In the case of model A, the components of each spin $\mathbf{s}_k$ in the Hamiltonian (H^A, Eq. 1) refer to local reference frames, with the x_k axis pointing in the radial direction. The general reference frame is chosen such that $\hat{\mathbf{r}}_1 = \hat{\mathbf{x}}$, being $\mathbf{r}_k$ the position of $\mathbf{s}_k$. (b) In the case of model B, the local reference frames refer to each of the couplings between nearest neighbouring spins; the x and y components are thus defined for each bond, with $\hat{\mathbf{x}}_k \parallel (\mathbf{r}_{k+1} - \mathbf{r}_k)$. Therefore, the components of each $\mathbf{s}_k$ in the Hamiltonian (H^B, Eq. 5) refer to two local reference frames, one for the coupling with $\mathbf{s}_{k-1}$ and one for that with $\mathbf{s}_{k+1}$.

II. THE MODEL

In order to provide an intuitive picture of the spin ring symmetry, we introduce the anisotropic Heisenberg model in a twisted-spin representation. In particular, we consider the case where the spins $\mathbf{s}_i$ are located at the vertices of a regular polygon, and the directions of the coordinate axes are determined either by the position ($\mathbf{r}_i$) of each spin within the ring (model A) or by the direction of the bond between the exchange-coupled spins (model B). In the case of model A [Fig. 1(a)], the x_i component of spin $\mathbf{s}_i$ is along the radial direction ($\hat{\mathbf{r}}_i = \hat{\mathbf{x}}_i$, with the origin O corresponding to the center of the polygon), whereas the y_i axis is defined so as to form with x_i a left-handed reference frame in the polygon plane. In the

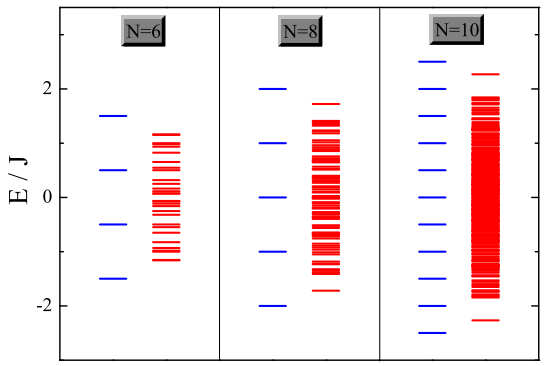

FIG. 2: (color online) Energy spectra of the noncollinear Ising Hamiltonians H^A_ξ (blue) and H^B_ξ (red) with N spins $s = 1/2$ and $\xi = X, Y$. For both model A and model B, the spectrum is independent on whether $J^\chi_{xx} = 0 \neq J^\chi_{yy}$ or $J^\chi_{yy} = 0 \neq J^\chi_{xx}$ and on the sign of the coupling. While the ground states of H^A_ξ are twofold degenerate, the ground doublets of H^B_ξ present the following splittings δ (not appreciable in the figure): $\delta/J \simeq 10^{-2}, 2.0 \times 10^{-4}, 10^{-5}$, for $N = 6, 8, 10$, respectively.

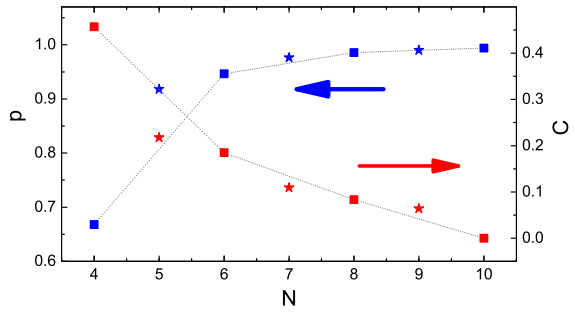

FIG. 3: (color online) Concurrence (red symbols, right axis) and squared modulus (blue symbols, left axis) of the overlap between the ground state of H^B_χ and the state $|\widetilde{\Psi}^\xi(\phi)\rangle$ (with $\xi = F, AF$ and $\chi = X, Y$; see Eq. 15). For even spin number (squares), the values of p and C are independent on the direction and sign of the coupling, but different angles ϕ are considered in the $\chi = Y$ ($\phi = 0$) and $\chi = X$ ($\phi = \pi/2$) cases. In the case of odd spin numbers (stars) the F cases have been considered.

case of model B [Fig. 1(b)], instead, the x components of two neighbouring and coupled spins, $\mathbf{s}_i$ and $\mathbf{s}_{i+1}$, are both along the side of the polygon $[\hat{\mathbf{x}}_i \parallel (\mathbf{r}_{i+1} - \mathbf{r}_i)]$.

A. Spin model A

In model A, the anisotropies in the Heisenberg coupling reflect the position of each spin within the ring:

$$H^A = \sum_{k=1}^{N} \left(J^A_{xx} s'_{k,x}\, s'_{k+1,x} + J^A_{yy} s'_{k,y}\, s'_{k+1,y} \right), \qquad (1)$$

where N is the number of spins and $\mathbf{s}_{N+1} \equiv \mathbf{s}_1$. The primed spin components can be expressed in terms of the general reference frame:

$$\begin{aligned} s'_{k,x} &= \mathbf{s}_k \cdot \hat{\mathbf{x}}^A_k = \cos\phi_k\, s_{k,x} + \sin\phi_k\, s_{k,y}, \\ s'_{k,y} &= \mathbf{s}_k \cdot \hat{\mathbf{y}}^A_k = \cos\phi_k\, s_{k,y} - \sin\phi_k\, s_{k,x}, \end{aligned} \qquad (2)$$

where $\hat{\mathbf{x}}^A_k = (\cos\phi_k, \sin\phi_k)$ and $\hat{\mathbf{y}}^A_k = (-\sin\phi_k, \cos\phi_k)$ in the xy basis, with $\phi_k = 2(k-1)\pi/N$. The Hamiltonian H^A can be thus rewritten in terms of the general reference frame:

$$H^A = \sum_{k=1}^{N} \sum_{\alpha,\beta=x,y} \left(J^{\alpha\beta}_k + D^{\alpha\beta}_k \right) s_{k,\alpha}\, s_{k+1,\beta}, \qquad (3)$$

where the tensors $\mathbf{J}$ and $\mathbf{D}$ account for the symmetric and antisymmetric components of the interaction ($J^{\alpha\beta}_k \equiv J^{\beta\alpha}_k$ and $D^{\alpha\beta}_k \equiv -D^{\beta\alpha}_k$), respectively:

$$\begin{aligned} J^{xx}_k &= J^A_{xx} \cos\phi_k \cos\phi_{k+1} + J^A_{yy} \sin\phi_k \sin\phi_{k+1}, \\ J^{yy}_k &= J^A_{yy} \cos\phi_k \cos\phi_{k+1} + J^A_{xx} \sin\phi_k \sin\phi_{k+1}, \\ J^{xy}_k &= \frac{1}{2}(J^A_{xx} - J^A_{yy}) \sin(\phi_{k+1} + \phi_k), \\ D^{xy}_k &= \frac{1}{2}(J^A_{xx} + J^A_{yy}) \sin(\phi_{k+1} - \phi_k), \end{aligned} \qquad (4)$$

while $D_{xx} = D_{yy} = 0$.

In the case $J^A_{xx} = J^A_{yy} \equiv J^A$, the couplings of the above Hamiltonian become site-independent, and they reduce to an isotropic symmetric contribution ($J^{xx}_k = J^{yy}_k = J^A \cos(2\pi/N)$ plus an antisymmetric one ($D^{xy}_k = J^A \sin(2\pi/N)$). In the following, we shall focus on the noncollinear Ising models H^A_X and H^A_Y, corresponding to $J^A_{yy} = 0 \neq J^A_{xx} \equiv J^A$ and $J^A_{xx} = 0 \neq J^A_{yy} \equiv J^A$, respectively. Both H^A_X and H^A_Y include, in the general reference frame representation, both (anisotropic) symmetric and antisymmetric terms, with components that depend on the spin index.

B. Spin model B

In model B, the preferential directions in the anisotropic Heisenberg model are determined by the direction of each bond:

$$H^B = \sum_{k=1}^{N} \left(J^B_{xx} s''_{k,x} s'''_{k+1,x} + J^B_{yy} s''_{k,y} s'''_{k+1,y} \right). \qquad (5)$$

Here, the components of each spin $\mathbf{s}_k$ are referred to two local reference frames: in the couplings with the spins

$\mathbf{s}_{k-1}$ and $\mathbf{s}_{k+1}$, these are (x_{k-1}, y_{k-1}) and (x_k, y_k), respectively:

$$\begin{aligned} s''_{k,x} &= \mathbf{s}_k \cdot \hat{\mathbf{x}}^B_k = \cos\varphi_k\, s_{k,x} + \sin\varphi_k\, s_{k,y}, \\ s''_{k,y} &= \mathbf{s}_k \cdot \hat{\mathbf{y}}^B_k = \cos\varphi_k\, s_{k,y} - \sin\varphi_k\, s_{k,x}, \\ s'''_{k+1,x} &= \mathbf{s}_k \cdot \hat{\mathbf{x}}^B_k = \cos\varphi_k\, s_{k+1,x} + \sin\varphi_k\, s_{k+1,y}, \\ s'''_{k+1,y} &= \mathbf{s}_k \cdot \hat{\mathbf{y}}^B_k = \cos\varphi_k\, s_{k+1,y} - \sin\varphi_k\, s_{k+1,x}, \end{aligned} \quad (6)$$

being $\hat{\mathbf{x}}^B_k = (\cos\varphi_k, \sin\varphi_k)$, $\hat{\mathbf{y}}^B_k = (-\sin\varphi_k, \cos\varphi_k)$ and $\varphi_k = \pi/2 + (2k-1)\pi/N$. In the general reference frame, the above Hamiltonian can be written as in Eq. 3, where:

$$\begin{aligned} J^{xx}_k &= J^B_{xx}\cos^2\varphi_k + J^B_{yy}\sin^2\varphi_k, \\ J^{yy}_k &= J^B_{yy}\cos^2\varphi_k + J^B_{xx}\sin^2\varphi_k, \\ J^{xy}_k &= (J^B_{xx} - J^B_{yy})\cos\varphi_k\,\sin\varphi_k, \\ D^{xy}_k &= 0. \end{aligned} \quad (7)$$

In the case $J^B_{xx} = J^B_{yy} \equiv J^B$, the couplings of H^B become site-independent, and only the symmetric and isotropic contribution is retained: $J^{xx}_k = J^{yy}_k = J^B$, with $J^{xy}_k = D^{xy}_k = 0$. In the following, we shall focus on the noncollinear Ising models H^B_X and H^B_Y, defined as $J^B_{yy} = 0 \neq J^B_{xx} \equiv J^B$ and $J^B_{xx} = 0 \neq J^B_{yy} \equiv J^B$, respectively. These cases correspond to a symmetric exchange ($D^{xy}_k = 0$), with the principal directions that vary from one spin pair to another.

We finally note that the above models A and B cannot, in general, be rephrased one in terms of the other. In fact, model A can be rewritten in the twisted-spin representation B only by adding an antisymmetric contribution:

$$\begin{aligned} J^B_{xx} &= -J^A_{xx}\sin^2(\pi/N) + J^A_{yy}\cos^2(\pi/N), \\ J^B_{yy} &= J^A_{xx}\cos^2(\pi/N) - J^A_{yy}\sin^2(\pi/N), \\ J^B_{xy} &= 0, \\ D^B_{xy} &= (J^A_{xx} + J^A_{yy})\cos(\pi/N)\sin(\pi/N). \end{aligned} \quad (8)$$

Analogous considerations apply to the model B in the twisted-spin representation A. In this case, the equations can be obtained from the above ones by swapping the A and B apices, and by changing the sign in the expression of the anti-symmetric exchange coefficient.

C. Symmetry properties of the A and B models

Both the A and B models belong to the $\mathbf{D}_{nh}$ point-group symmetry [13], with n corresponding to the spin number ($n = N$). In fact, one can show that H^A and H^B are invariant under N different $\hat{C}_2$ rotations $\exp(-i\mathbf{J}\cdot\hat{\mathbf{n}}_k\pi/\hbar)$, with $\mathbf{J} = \sum_{i=1}^N(\mathbf{l}_i + \mathbf{s}_i)$: $N/2$ rotations have axes parallel to the spin positions, $\hat{\mathbf{n}}_k = \mathbf{r}_k$ with $k = 1, 2, \ldots, N/2$; the other $N/2$ rotations have axes that coincide with the bisectors of the polygon sides, $\hat{\mathbf{n}}_k = (\mathbf{r}_k + \mathbf{r}_{k+1})/|\mathbf{r}_k + \mathbf{r}_{k+1}|$, with $k = N/2+1, \ldots, N$.

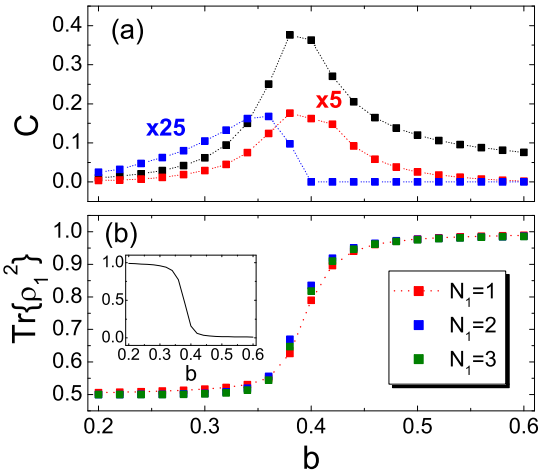

FIG. 4: (color online) Quantum entanglement in an hexagonal ring of $s = 1/2$ spins, model H^A_X with $J^A_{xx} = -1$, in the presence of an external magnetic field $\mathbf{b} = b\hat{\mathbf{x}}$. (a) Pairwise entanglement, quantified by the concurrence (C) between the spins $\mathbf{s}_k$ and $\mathbf{s}_l$, with $|k-l| = 1$(black squares), 2 (red, multiplied by a factor 5), 3 (blue, factor 25). (b) Block entanglement between subsystems $\mathcal{S}_1$ and $\mathcal{S}_2$, (consisting of N_1 and $N_2 = N - N_1$ consecutive spins, respectively), quantified by $\mathrm{Tr}(\rho_1^2)$, with ρ_1 the reduced density matrix of $\mathcal{S}_1$. Inset: Residual tangle of the single spin.

The Hamiltonians H^A and H^B are also invariant under reflection ($\hat{\sigma}_h$) about the polygon plane xy, and under the $\hat{C}_n$ rotation $\exp(-i2\pi J_z/N\hbar)$ around the vertical axis z. We note that the collinear XY model, $H_{XY} = J_{xx}\sum_{k=1}^N(s_{k,x'}s_{k+1,x'} + s_{k,y'}s_{k+1,y'})$, belongs to the $\mathbf{D}_{2h}$ point-group symmetry, if the x' and y' axes coincide with symmetry axes of the polygon defined by the spin positions, i.e. if $\hat{\mathbf{x}}'$ and $\hat{\mathbf{y}}'$ are parallel to two of the $\hat{\mathbf{n}}_k$. In the following we shall assume for simplicity that this is the case, and in particular that $\hat{\mathbf{x}}' = \hat{\mathbf{x}}$ and $\hat{\mathbf{y}}' = \hat{\mathbf{y}}$.

As suggested by the high degree of degeneracy of its energy spectrum (see below), the collinear Ising models H_X and H_Y are also invariant under a number of additional transformations, that apply to the orbital or spin degrees of freedom separately. In the case of the hexagon (Fig. 1), for example, the symmetry operations of $H_{\xi=X,Y}$ include all the elements of the $\mathbf{D}_{6h}$ group, where each transformation is applied to the orbital part only: 6 different $\hat{C}_2$ rotations $\exp(-i\mathbf{L}\cdot\hat{\mathbf{n}}_k\pi/\hbar)$, with $\mathbf{L} = \sum_{i=1}^N \mathbf{l}_i$ and the 6 rotations axes $\hat{\mathbf{n}}_k$ defined as above; reflection about the polygon plane xy; $\hat{C}_n$ rotation $\exp(-i2\pi L_z/N\hbar)$ around the vertical axis z, whih can be thought as the analogue of translational invariance for a system with periodic boundary conditions. If we assume for simplicity that the electrons occupy spherically symmetric orbitals centered at the positions $\mathbf{r}_i$, the

transformations of $\mathbf{D}_{6h}$ simply result in permutations of the spin indices. The rotation of an angle $\pi/3$ around the z axis, e.g., induces the following transformations: $(s_{k,x}, s_{k,y}, s_{k,z}) \longrightarrow (s_{k+1,x}, s_{k+1,y}, s_{k+1,z})$. In general, one can show that the H_{XY} Hamiltonian of an N-spin regular polygon is invariant under transformations belonging to the $\mathbf{D}_{nh}$ group (with $n = N$). The models A and B, instead, are only invariant under reflection of the orbital degrees of freedom about the xy plane.

As far as spin transformations are concerned, the collinear XY model belongs to the $\mathbf{D}_{2h}$ group, with the C_2 axes that coincide with the x' and y' axes. The $\hat{C}_2$ rotations thus correspond to $\exp(-iS_\alpha\pi/\hbar)$, with $\mathbf{S} = \sum_{i=1}^{N} \mathbf{s}_i$ and $\alpha = x', y', z$. The collinear Ising model H_X (H_Y) is additionally invariant with respect to continuous spin rotations around the x' (y') axis. The Hamiltonians H_A and H_B, instead, are only invariant under reflection about the xy plane, corresponding to the transformation: $(s_{k,x}, s_{k,y}, s_{k,z}) \longrightarrow (-s_{k,x}, -s_{k,y}, s_{k,z})$. We finally note that the Hamiltonians H^A_ξ and $H_{\xi'}$ ($\xi, \xi' = X, Y$) are unitarily equivalent: $H^A_\xi = \mathcal{U}_{\xi\xi'} H_{\xi'} \mathcal{U}^{-1}_{\xi\xi'}$. In the case $\hat{\mathbf{x}}' = \hat{\mathbf{x}}$, for example, $\mathcal{U}_{XX} = \otimes_{k=1}^{N} \exp(-is_{k,z}\phi_k/\hbar)$. Therefore, one can associate the symmetry operation $\mathcal{U}_{\xi\xi'}C$ of $H_{\xi'}$ to any symmetry operation of C of H^A_ξ (and vice versa). As shown below, the collinear and noncollinear models become significantly different (i.e. no longer unitarily equivalent) in the presence of an applied magnetic field.

III. RESULTS

A. Energy spectra and trial wavefunctions

The results presented below are based on the direct diagonalization of the Hamiltonians H^A and H^B for rings of $s = 1/2$ spins. The energy spectra of the noncollinear Ising models (Fig. 2) are independent on whether $J_{xx} \neq 0 = J_{yy}$ ($H^A = H^A_X$) or $J_{yy} \neq 0 = J_{xx}$ ($H^A = H^A_Y$), and coincide with those of the collinear Ising model ($H_{\xi=X,Y}$). As already mentioned in the previous section, all these models are in fact unitarily equivalent. The twofold degenerate ground states of H^A_ξ, like any other eigenstate $|\Psi^A_k\rangle$, can be derived from those of $H_{\xi'}$ by the unitary transformation $\mathcal{U}_{\xi\xi'}$:

$$|\beta^\chi_k(\phi)\rangle = \mathcal{U}_{\xi\xi'}|\alpha^\chi_x\rangle = \left[\otimes_{l=1}^{N} R^l_z(\phi_l + \phi + k\pi)\right]|\alpha^\chi_x\rangle, \quad (9)$$

where $R_{k,z}(\varphi) = \exp(-is_{k,z}\varphi)$, $\phi = \phi(\xi, \xi')$, and $k = 0, 1$. The expression of $|\alpha^\chi_x\rangle$ depends on whether the coupling has a ferromagnetic ($\chi = F$) or an antiferromagnetic ($\chi = AF$) character:

$$\begin{aligned} |\alpha^F_x\rangle &= |\uparrow_x\uparrow_x \ldots \uparrow_x\uparrow_x\rangle, \\ |\alpha^{AF}_x\rangle &= |\uparrow_x\downarrow_x \ldots \uparrow_x\downarrow_x\rangle, \end{aligned} \quad (10)$$

where $|\uparrow_x\rangle$ and $|\downarrow_x\rangle$ are the eigenstates of the single-spin projection along the x direction. Finally, one can easily verify that $\phi = 0$ for $\xi = \xi'$, whereas $\phi = \pm\pi/2$ if (ξ, ξ') coincides with (Y, X) or (X, Y), respectively.

The spectrum of H^B_ξ is characterized by a lower degree of degeneration with respect to that of H^A_ξ (Fig. 2), reflecting the lower symmetry of the former Hamiltonian with respect to the latter one. In particular, the ground state doublet presents a splitting δ, whose magnitude decreases with the number of spins, as reported in the figure caption. For each spin ring, the energy spectrum is independent on whether $H^B = H^B_X$ or $H^B = H^B_Y$ and on the sign of the coupling J^B. In fact, all these Hamiltonians are unitarily equivalent, being:

$$H^B_Y = \mathcal{U}\, H^B_X\, \mathcal{U}^{-1}, \text{ with } \mathcal{U} = \otimes_{k=1}^{N} e^{-i\pi s_{k,z}/2}, \quad (11)$$

$$H^B_X = \mathcal{U}\,(-H^B_X)\,\mathcal{U}^{-1}, \text{ with } \mathcal{U} = \otimes_{k=1}^{N/2} e^{-i\pi s_{2k,z}}, \quad (12)$$

where the latter equation also implies that the energy spectrum is symmetric with respect to the origin. In the following we thus refer, without loss of generality, to the case of H^B_X with $J^B_X > 0$. In all the considered cases, it was found that the ground state H^B_X could be expressed as a linear combinations of a limited number of symmetry-adapted states:

$$|\Psi^B_0\rangle = \left[\otimes_{l=1}^{N} R_{l,z}(\phi_l)\right] \sum_{k=0}^{N/2} \sum_{\{\mathbf{v}_k\}} C^{\mathbf{v}_k}_k |\Phi^{\mathbf{v}_k}_k\rangle, \quad (13)$$

where the total spin projection along z of each component is fixed by k ($M = N/2 - 2k$). The components $|\Phi^{\mathbf{v}_k}_k\rangle$, whose coefficients $C^{\mathbf{v}_k}_k$ are determined numerically, are given by

$$|\Phi^{\mathbf{v}_k}_k\rangle = (-1)^{\sum_p v^k_p} \sum_n \left(\otimes_{q=1}^{2k} \sigma_{v^k_q + n, x}\right) |\alpha^F_z\rangle, \quad (14)$$

where the $2k$ elements $1 \leq v^k_p \leq N$ of the vector $\mathbf{v}_k$ specify which spins are flipped with respect to the reference configuration $|\alpha^F_z\rangle = |\uparrow_z\uparrow_z \ldots \uparrow_z\uparrow_z\rangle$. In Eq. 14, different vectors $\mathbf{v}_k$ correspond to components that cannot be transformed one into another by rotating the spin ring of an angle ϕ_l around the z axis. For example, the components of $|\Phi^{\mathbf{v}_1}_1\rangle$ and $|\Phi^{\mathbf{v}_2}_1\rangle$ can be represented by all the states where the only two down spins are nearest neighbours or next nearest neighbours, respectively. In the case $J_X < 0$, the state $|\alpha^F_z\rangle$ in Eq. 14 is replaced by its antiferromagnetic counterpart $|\alpha^{AF}_z\rangle$. Besides, additional relations are found between the coefficients of $|\Phi^{\mathbf{v}_k}_k\rangle$ and $|\Phi^{\tilde{\mathbf{v}}_k}_{N/2-k}\rangle$, that are the spin-flipped versions of one another, depending on the model, direction and character (ferromagnetic or antiferromagnetic) of the coupling (Table I). The use of the expression 13 as a trial wavefunction for the ground state allows to reduce drastically the dimension of the Hamiltonian to be diagonalized, for example from 256 to 12 for $N = 8$ spins $s = 1/2$, or from 1024 to 15 for $N = 10$.

$C_k^{\mathbf{v}_k}/C_k^{\tilde{\mathbf{v}}_{N/2-k}}$	$J_{xx}>0$	$J_{xx}<0$	$J_{yy}>0$	$J_{yy}<0$
model A	-1	1	1	-1
model B	1	-1	-1	1

TABLE I: Ratio between the coefficients $C_k^{\mathbf{v}_k}$ and $C_k^{\tilde{\mathbf{v}}_{N/2-k}}$ in the ground state of the noncollinear Ising models B. The components $|\Phi_k^{\mathbf{v}_k}\rangle$ and $|\Phi_{N/2-k}^{\tilde{\mathbf{v}}_k}\rangle$ in Eq. 13 are the spin-flipped versions of one another.

B. Ground state entanglement without field

Unlike the standard Ising model, the noncollinear one (H_X^B) presents remarkable entanglement properties in the absence of an external magnetic field. In fact, we find that the ground state of H^B approximately corresponds to a symmetric combination of the two degenerate ground states of H^A:

$$|\widetilde{\Psi}^{\xi}(\phi)\rangle = \frac{1}{\sqrt{2}}\left[|\beta_0^{\xi}(\phi)\rangle + |\beta_1^{\xi}(\phi)\rangle\right], \qquad (15)$$

where $\phi = \pi/2$ and $\xi = F$ ($\xi = AF$) for J_{xx}^B negative (positive). As reported in Fig. 3 (filled blue squares), the squared modulus of such overlap, $p = |\langle\Psi_0^B|\widetilde{\Psi}^{\xi}\rangle|^2$, increases with the spin number N and approaches 1 already for $N = 10$. As a consequence, the ground state of the noncollinear Ising model B essentially corresponds to a linear superpositions of macroscopically different components, where the state of each spin in $|\beta_0^{\xi}(\phi)\rangle$ is orthogonal to the state of the same spin in $|\beta_1^{\xi}(\phi)\rangle$. In analogy with the magnetization and Néel vectors, whose coherent tunneling is expected to take place in the ground state of molecular nanomagnets with ferromagnetic and antiferromagnetic Heisenberg interaction, respectively [14], we introduce here the vectors $\mathbf{n}_F$ and $\mathbf{n}_{AF}$, defined as:

$$\mathbf{n}_F(\phi) = \frac{1}{Ns}\sum_{k=1}^{N}\left\{R_{k,z}^{-1}(\phi_k+\phi)\,\mathbf{s}_k\,R_{k,z}(\phi_k+\phi)\right\} \qquad (16)$$

$$\mathbf{n}_{AF}(\phi) = \sum_{k=1}^{N}\frac{(-1)^k}{Ns}\left\{R_{k,z}^{-1}(\phi_k+\phi)\,\mathbf{s}_k\,R_{k,z}(\phi_k+\phi)\right\}. \qquad (17)$$

These vectors have maximum modulus and opposite orientations in the case of the two macroscopically different components in Eq. 15: $|\langle\beta_0^{\xi}(\phi)|\mathbf{n}_{\xi}(\phi)|\beta_0^{\xi}(\phi)\rangle| = 1$ and $\langle\beta_0^{\xi}(\phi)|\mathbf{n}_{\xi}(\phi)|\beta_0^{\xi}(\phi)\rangle = -\langle\beta_1^{\xi}(\phi)|\mathbf{n}_{\xi}(\phi)|\beta_1^{\xi}(\phi)\rangle$, with $\xi = F, AF$. We can thus summarize the result reported in Fig. 3 by saying that the ground state of the noncollinear Ising models H_X^B presents coherent tunneling of the vectors $\mathbf{n}_{\xi}(\pi/2)$.

Similar results can be found in the case of odd spin numbers. Here, the overall Hilbert space can be divided into two uncoupled subspaces, including either the states with $M = -N/2 + 2(k-1)$, or those with $M = +N/2 - 2(k-1)$ (being $k = 1, 2, \ldots, N/2$). This results in a twofold degeneracy of all eigenvalues. Besides, the ferromagnetic and antiferromagnetic cases are no longer equivalent, and an additional degeneracy of the ground state is induced by spin frustration in the latter case. In Fig. 3, we report the squared modulus of the overlap $\langle\Psi_0^B|\widetilde{\Psi}^F\rangle$ for odd N (stars), where $|\Psi_0^B\rangle$ is obtained by diagonalizing H_X^B within each of the above mentioned subspaces. The trend as a function of N resembles that obtained for even spin numbers. The possibility of approximating the ground state of H^B with the state $|\widetilde{\Psi}^{\xi}(\phi)\rangle$ applies also to spins $s > 1/2$. In these cases, the single-spin states $|\uparrow_x\rangle$ and $|\downarrow_x\rangle$ that enter the definition of $|\alpha_x^{\chi}\rangle$ (Eq. 10) correspond to $|m_x = +s\rangle$ and $|m_x = -s\rangle$, respectively. For example, from analogous calculations performed on $s = 1$ spins (not reported here) the overlap between the ground state of H^B and $|\widetilde{\Psi}^{\xi}(\phi)\rangle$ is larger than for rings of 1/2 spins with equal N.

From the point of view of quantum correlations, the states $|\widetilde{\Psi}^{\xi}\rangle$ are equivalent to the Greenberger-Horne-Zeilinger (GHZ) states, characterized by a genuine multipartite entanglement and by vanishing pairwise entanglement. Pairwise entanglement between nearest neighbouring spins is however present in the ground state of H_X^B. In fact, the concurrence between nearest neighbours has finite values (red squares in Fig. 3), that decrease for increasing N, and tend to zero as the ground state tends to the GHZ-like state $|\widetilde{\Psi}^{\xi}(\phi)\rangle$. The concurrence between

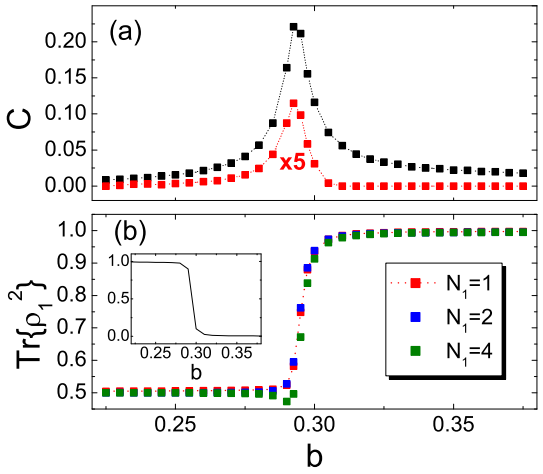

FIG. 5: (color online) Quantum entanglement in an octagonal ring of $s = 1/2$ spins, model H_X^A with $J_{xx}^A = -1$, in the presence of an external magnetic field $\mathbf{b} = b\hat{\mathbf{x}}$. (a) Pairwise entanglement, quantified by the concurrence (C) between the spins $\mathbf{s}_k$ and $\mathbf{s}_l$, with $|k-l| = 1$ (black squares), 2 (red, multiplied by a factor 5). (b) Block entanglement between subsystems $\mathcal{S}_1$ and $\mathcal{S}_2$, (consisting of N_1 and $N_2 = N - N_1$ consecutive spins, respectively), quantified by $\mathrm{Tr}(\rho_1^2)$, with ρ_1 the reduced density matrix of $\mathcal{S}_1$. Inset: Residual tangle of the single spin.

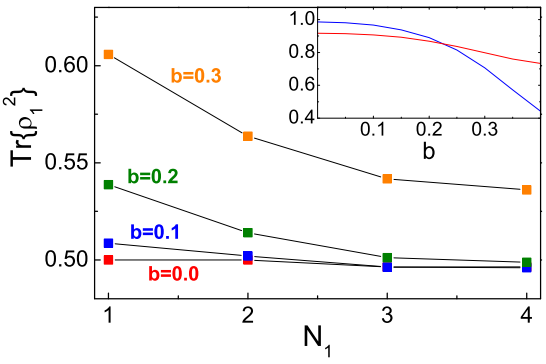

FIG. 6: (color online) (color online) Entanglement between two subsystems of consecutive spins ($\mathcal{S}_1$ and $\mathcal{S}_2$) quantified by $\mathrm{Tr}(\rho_1^2)$, being ρ_1 the reduced density matrix of $\mathcal{S}_1$. The trace is computed for the ground state of $H^B + H_b^B$, and is displayed as a function of the number of spins of $\mathcal{S}_1$, $N_1 = N - N_2$, in the case $N = 8$ and for different values of the magnetic field. Inset: Residual tangle (blue curve) and concurrence C (plotted as $1 - C$, red) as a function of the magnetic field b.

pairs of spins that aren't nearest neighbours (not shown) is zero in all the considered cases.

C. Magnetic field induced entanglement

The magnetic field can be used as a control parameter in order to tune the quantum correlations within the ring. In the case of model A, the two degenerate and separable ground states $|\beta_k^\chi(\phi)\rangle$ can be coupled by applying an homogeneous in-plane magnetic field $H_b^A = b\sum_{k=1}^N s_{k,x}$. As a result, the degeneracy is removed, and $|\Psi_0^A\rangle$ tends to a linear superposition of macroscopically distinct states. The overlap between the ground state and $|\widetilde{\Psi}^\xi(\phi)\rangle$ (Eq. 15) as a function of the magnetic field is reported in Fig. 4 ($N = 6$) and Fig. 5 ($N = 8$). The in-plane magnetic field reduces the symmetry of the system and breaks the equivalence between the noncollinear Ising models H_ξ^A and their collinear counterparts, and that between the ferromagnetic and antiferromagnetic cases. One of the consequences of the symmetry reduction is the removal of the degeneracy in the ground state. In fact, the energy splitting $\delta = E_1 - E_0$ between ground and first excited states, increases with b (not shown). The field however also mixes the subspace spanned by $|\beta_0^\chi(\phi)\rangle$ and $|\beta_1^\chi(\phi)\rangle$ with additional components, thus reducing the overlap between $|\Psi_0^A\rangle$ and $|\widetilde{\Psi}^\xi(\phi)\rangle$ (see Table II). All this is reflected in the entanglement properties of the ground state. For low values of the field, the concurrence between all pairs of spins is negligible [Figs. 4(a) and 5(a)], whereas any blocks of N_1 consecutive spins is entangled with the complementary block of $N_2 = N - N_1$ (panels (b)). Moreover, the value of $\mathrm{Tr}(\rho_1^2)$ is close to $1/2$, independently on the partition (N_1). Finally, the residual tangle, that quantifies the genuine multipartite entanglement and is defined as $4\det(\rho_k) - \sum_{i\neq k} C_{ik}^2$ (with ρ_k the reduced density matrix of the k-th spin C_{ik} the concurrence between spins i and k), is maximized (insets). All these features are consistent with a GHZ-like form of the ground state. For high values of the field, the ground state tends to a factorizable form, as shown by the simultaneous suppression of pairwise, block and multipartite entanglement. In the intermediate region ($b \simeq 0.4$ for $N = 6$ and $b \simeq 0.3$ for $N = 8$), the abrupt reduction of the residual tangle and of the block entanglement is accompanied by peaks in the values of the concurrence, not only between nearest neighbours.

We note in passing that the noncollinear Ising H_X^A, combined with an homogeneous magnetic field, results in an Hamiltonian and in ground state entanglement properties that are equivalent to those of a collinear Ising interaction in the presence of an inhomogeneous magnetic field, with radial field orientation at each spin site ($\mathbf{b}_k \parallel \mathbf{r}_k$). While the latter geometry might produce remarkable entanglement properties in mesoscopic (pseudo)spin systems [11], the former one seems much more suitable for producing analogous effects in nanometer-sized objects, such as molecular nanomagnets.

In the case of model B, we consider a magnetic field applied along the z direction, giving rise to an additional term in the Hamiltonian: $H_b^B = b\sum_{k=1}^N s_{k,z}$. Such field preserves the equivalence between the ferromagnetic ($J_{xx}^B < 0$) and antiferromagnetic ($J_{xx}^B > 0$) models, as well as that between the $J_{xx}^B = 0$ and $J_{yy}^B = 0$ cases. We find that, also in the presence of the field, the ground state of the noncollinear Ising model B is well approximated by a linear superposition of two macroscopically different states:

$$|\widetilde{\Psi}_t^\xi(\theta,\phi)\rangle = \frac{1}{\sqrt{C}}\left[|\gamma_0^\xi(\theta,\phi)\rangle + |\gamma_1^\xi(\theta,\phi)\rangle\right], \qquad (18)$$

where

$$|\gamma_k^\xi(\theta,\phi)\rangle = \left[\otimes_{l=1}^N R_{l,z}(\phi_l + \phi + k\pi)\right]|\alpha_t^\xi(\theta)\rangle. \qquad (19)$$

Here $\xi = F$ or $\xi = AF$, depending on whether the coupling has a ferromagnetic or an antiferromagnetic character:

$$\begin{aligned} |\alpha_t^F(\theta)\rangle &= \left[\otimes_{q=1}^N R_{q,y}(\theta)\right]|\uparrow_z\uparrow_z\ldots\uparrow_z\rangle, \\ |\alpha_t^{AF}(\theta)\rangle &= \left\{\otimes_{q=1}^N R_y^q[(-1)^q\theta]\right\}|\uparrow_z\uparrow_z\ldots\uparrow_z\rangle. \end{aligned} \qquad (20)$$

Unlike $|\beta_0^\xi(\phi)\rangle$ and $|\beta_1^\xi(\phi)\rangle$ (Eq. 9), the states $|\gamma_0^\xi(\theta,\phi)\rangle$ and $|\gamma_1^\xi(\theta,\phi)\rangle$ are not mutually orthogonal, unless $\theta = \pi/2$, so that $|\alpha_t^F(\theta)\rangle = |\alpha_x^F(\theta)\rangle$ and $|\gamma_k^\xi(\theta,\phi)\rangle = |\beta_k^\xi(\phi)\rangle$. In general, $|\langle\gamma_0^\xi(\theta,\phi)|\gamma_1^\xi(\theta,\phi)\rangle| = |\cos\theta|^N$; the normalization constant in Eq. 18 is thus $C = 2(1 + |\cos\theta|^N)$. As detailed in Table II, for increasing values of the field,

$b\,(\mathbf{b} \parallel \hat{\mathbf{x}})$		0.2	0.225	0.25	0.275	0.3
model	p	0.956	0.947	0.936	0.913	0.0595
A	θ_M/π	0.5	0.5	0.5	0.5	0.5
$b\,(\mathbf{b} \parallel \hat{\mathbf{z}})$		0	0.1	0.2	0.3	0.4
model	p	0.985	0.980	0.960	0.909	0.862
B	θ_M/π	0.250	0.229	0.206	0.173	0.136

TABLE II: Square modulus p of the overlap between the trial wavefunction $|\widetilde{\Psi}_t^{\xi}(\theta,\phi)\rangle$ and ground state of $H^A + H_b^A$ (upper lines) or $H^B + H_b^B$ (lower lines), with $N = 8$. The angle θ_M is the value of θ that maximizes p. In the case of the models A and B, the magnetic field is oriented along the x and z directions, respectively. The above results refer to H_X^A, with $J_{xx}^A = -1$; as to the model B, no difference emerges between $H_X^B + H_b^B$ and $H_Y^B + H_b^B$, nor between $J_{xx}^B = +1$ and $J_{xx}^B = -1$.

the overlap between $|\Psi_0^B\rangle$ and $|\widetilde{\Psi}_t^{\xi}(\theta,\phi)\rangle$ decreases, while the value θ_M of the angle θ that maximizes such overlap decreases. As θ_M passes from $\pi/2$ (like in the case $b = 0$) to lower values, the entanglement properties of the ground state deviate from those of a GHZ state (Fig. 6). In particular, the entanglement between a block of N_1 consecutive spins and the remaining $N_2 = N - N_1$ ones, quantified by $\mathrm{Tr}\{\rho_1^2\}$, becomes an increasing function of the N_1, whereas for $b = 0$ it is practically independent on N_1, as for a GHZ state. The pairwise entanglement between nearest neighbouring spins, quantified by the concurrence, increases (red curve, figure inset). The multipartite entanglement, as quantified by the residual tangle, decreases for increasing b (blue curve). Altogether, the perpendicular magnetic field thus induces a transition from a predominantly multipartite entangled ground state to one with large pairwise quantum correlations.

IV. CONCLUSIONS

In conclusion, we have investigated spin rings that are coupled by noncollinear Ising interactions, whose anisotropy reflects the point-group symmetry of the system. The ground states of these Hamiltonians exhibit remarkable entanglement properties. In particular, in the case where the preferential directions for each spin are determined by the direction of the spin-spin bond (model B), the system ground state $|\Psi_0^B\rangle$ is characterized by a large multipartite entanglement and by a low degree of pairwise entanglement. In fact, the overlap between $|\Psi_0^B\rangle$ and a GHZ-like state increases with the number of spins N, and approaches 1 already for $N = 10$. A vertical magnetic field can be used to substantially modify such picture, enhancing the pairwise entanglement between nearest neighbouring spins at the expense of multipartite entanglement. In the case where the preferential directions for each spin are determined solely by its position within the ring (irrespective of the bond direction) - model A - the noncollinear Ising Hamiltonian is unitarily equivalent to the standard Ising model, and thus the degenerate ground state doublet is spanned by two factorizable states. However, the application of an moderate (with respect to J) in-plane field splits such doublet and induces multipartite entanglement in the ground state $|\Psi_0^A\rangle$. For increasing values of the field, $|\Psi_0^A\rangle$ undergoes a sharp transition towards a separable ferromagnetic ground state, accompanied a peak in the pairwise entanglement, not only between nearest neighbouring spins. While these results have been obtained for $s = 1/2$ spins, analogous behaviours emerge from preliminary calculations performed with higher spin values.

[1] L. Amico, R. Fazio, A. Osterloh, and V. Vedral, Rev. Mod. Phys. **80**, 517 (2008).
[2] R. Horodecki, P. Horodecki, M. Horodecki, and K. Horodecki, Rev. Mod. Phys. **81**, 865 (2009).
[3] K. M. O'Connor and W. K. Wootters, Phys. Rev. A **63**, 052302 (2001).
[4] J. Kurmann, H. Thomas, and G. Mller, Physica A: Statistical and Theoretical Physics **112**, 235 (1982).
[5] S. M. Giampaolo, G. Adesso, and F. Illuminati, Phys. Rev. Lett. **100**, 197201 (2008).
[6] N. Canosa, R. Rossignoli, and J. M. Matera, Phys. Rev. B **81**, 054415 (2010).
[7] R. Rossignoli, N. Canosa, and J. M. Matera, Phys. Rev. A **77**, 052322 (2008).
[8] L. Amico, F. Baroni, A. Fubini, D. Patanè, V. Tognetti, and P. Verrucchi, Phys. Rev. A **74**, 022322 (2006).
[9] S. M. Giampaolo, F. Illuminati, P. Verrucchi, and S. De Siena, Phys. Rev. A **77**, 012319 (2008).
[10] T. Roscilde, P. Verrucchi, A. Fubini, S. Haas, and V. Tognetti, Phys. Rev. Lett. **93**, 167203 (2004).
[11] B. Röthlisberger, J. Lehmann, D. S. Saraga, P. Traber, and D. Loss, Phys. Rev. Lett. **100**, 100502 (2008).
[12] R. Rossignoli, N. Canosa, and J. M. Matera, Phys. Rev. A **80**, 062325 (2009).
[13] B. Tsukerblat, *Group theory in chemistry and spectroscopy* (Academic Press, New York, 1994).
[14] D. Gatteschi, R. Sessoli, and J. Villain, *Molecular nanomagnets* (Oxford University Press, 2007).
[15] F. Troiani, M. Affronte, S. Carretta, P. Santini, and G. Amoretti, Phys. Rev. Lett. **94**, 190501 (2005).
[16] M. Trif, F. Troiani, D. Stepanenko, and D. Loss, Phys. Rev. Lett. **101**, 217201 (2008).
[17] F. Troiani, A. Ghirri, M. Affronte, S. Carretta, P. Santini, G. Amoretti, S. Piligkos, G. Timco, and R. E. P. Winpenny, Phys. Rev. Lett. **94**, 207208 (2005).
[18] J. Luzon, K. Bernot, I. J. Hewitt, C. E. Anson, A. K. Powell, and R. Sessoli, Phys. Rev. Lett. **100**, 247205 (2008).
[19] V. S. Mironov, L. F. Chibotaru, and A. Ceulemans, J. Am. Chem. Soc. **125**, 9750 (2003).